Nano-ZnO film preparation at low temperature and the optical indices calculation*

YANG Ai-ling (杨爱玲)[1]**, **BAO Xi-chang** (包西昌)[2], **LI Shun-pin** (李顺嫔)[1], **YANG Ren-qiang** (阳仁强)[2], **WANG Ting** (王婷)[2], **WANG Yu-jin** (王玉金)[1], and **SUN Liang** (孙亮)[2]

1. Department of Physics, Ocean University of China, Qingdao 266100, China

2. Qingdao Institute of Bioenergy & Bioprocess Technology, Chinese Academy of Sciences, Qingdao 266101, China

(Received 11 March 2014)

The refractive indices of thin films based on Kramers-Kronig theory are corrected. And the correction theory is used to determine the optical indices of nano-ZnO thin films prepared by low temperature sol-gel method. The calculated results indicate that in the visible (Vis) range, the refractive indices of nano-ZnO thin films exhibit a slight abnormal dispersion, while in the ultraviolet (UV) region, the refractive indices increase with wavelengths increasing (normal dispersion). But the refractive indices show complex change near the absorption edge. The maximum refractive index (1.95) of nano-ZnO thin films within UV range at low temperature annealing is much lower than that of the films annealed at high temperature. The absorption and refractive indices are closely related to the defects in nano-ZnO thin films.

Document code: A **Article ID:** 1673-1905(2014)03-0216-5

DOI 10.1007/s11801-014-4034-6

ZnO is very important for its potential applications in electronic and optoelectronic devices[1], such as laser diode[2], light emitting devices[3,4], display device[5], field emission[6,7], optical detector in UV range[8-10], microsensors[11-13], solar cells[14-16], photocatalysis[17,18] and fluorescence enhancing[19,20].

Optical constants of nano-ZnO films, such as absorption coefficient, refractive index, extinction coefficient and complex dielectric constant, are important parameters for the applications in relative device design. The refractive index is closely related to the electronic polarizability of ions and local field inside materials[21]. Under higher annealing temperature, the effects of annealing temperature on the refractive indices of nano-ZnO films have been reported[21-23]. Some groups have developed different methods to calculate the optical constants of ZnO or doped ZnO thin films[24,25]. In recent years, the synthesis of nano-ZnO thin films at low temperature[26-28] is noted for their potential applications as electron transport layers in flexible organic devices. In this paper, nano-ZnO thin films were prepared by low temperature sol-gel method. Transmission spectra and scanning electron microscope (SEM) results of these films were characterized. We find that there are some errors with Xue's[24] theory based on Kramers-Kronig relationship to calculate refractive index of thin films. We correct these errors, and the optical indices of nano-ZnO thin films are calculated.

The sol-gel method similar to Ref.[26] but with a little change is used to prepare ZnO nanoparticles. The 2-ethoxyethanol is as the solvent. The molar ratio between zinc acetate 2-hydrate ($Zn(CH_3COO)_2 \cdot 2H_2O$) and monoethamine (MEA) is 1:1. Two concentrations of zinc acetate 2-hydrate (0.5 mol/L and 1.0 mol/L) are chosen and the mixtures were stirred at 50 °C for 60 min to produce clear homogeneous solutions. Then the solutions were spin-coated with 500 r/min, 1000 r/min and 2000 r/min successively for 30 s on quartz glass. After spin-coating, the films were annealed at 100 °C in an oven for 30 h. Subsequently, nano-ZnO films with different zinc concentrations and thicknesses were prepared. Tab.1 shows the concrete preparation conditions and parameters of the samples.

Tab.1 Preparation conditions and parameters of nano-ZnO thin films

Sample	Concentration of zinc ions (mol/L)	Spin coating speed (r/min)	Average thickness (nm)
A	0.5	500	107
B	0.5	1000	65
C	1.0	500	253
D	1.0	1000	167
E	1.0	2000	122

* This work has been supported by the National Natural Science Foundation of China (Nos.41172110 and 61107090) and Shandong Provincial Natural Science Foundation (No.ZR2011BZ007).

** E-mail: ailingy@ouc.edu.cn

The morphologies of nano-ZnO films were characterized by scanning electron microscopy (SEM, Hi-tachi4800). A Cary-50 UV-Vis spectrophotometer was used to measure the absorption spectra. The thicknesses of the films were measured by a Veeco Dektak150 surface profiler.

The X-ray diffraction (XRD) patterns are similar to our former results[28]. Fig.1 shows the representative SEM image of sample D. We can see that the sizes of the nanoparticles are in the range of 10—16 nm. The nano-ZnO thin film is homogenous and smooth. The film quality is good.

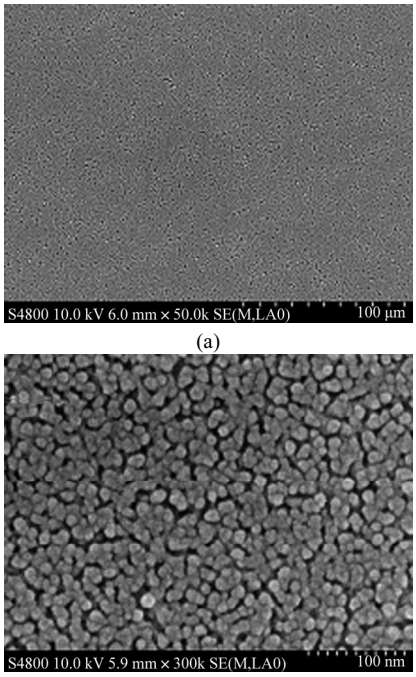

Fig.1 (a) SEM image of nano-ZnO thin film (sample D); (b) Magnified image of (a)

Fig.2 shows the transmission curves of the five nano-ZnO thin films. In the UV range, the order of transmittances of the five samples is B>A>E>D>C, which is consistent with the thickness order of the samples. But in the visible range, the transmittance of B, A, E and D samples is up to 90% and has little difference, while the transmittance of sample C is slightly lower (~85%) than that of the others. The reason is that the thickness of sample C is the largest among the five samples.

The refractive index $n(\lambda)$ of a thin film is related to the absorption coefficient $\alpha(\lambda)$ from Kramers-Kronig equation, that is

$$n(\lambda)-1=\frac{1}{2\pi^2}\int_0^{\infty}\frac{\alpha(\lambda')\mathrm{d}\lambda'}{1-\lambda'^2/\lambda^2}. \tag{1}$$

According to Eq.(1), for calculation $n(\lambda)$, one should know $\alpha(\lambda')$ in the range of 0—∞. But one can only obtain $\alpha(\lambda')$ in a limited wavelength range ($\lambda_1'\sim\lambda_2'$) from transmittance spectrum. In our experiment, this wavelength range is 300—700 nm. In the regions of λ_1'<300 nm and λ_2'>700 nm, one has to guess $\alpha(\lambda')$. So Eq.(1) can be written as

$$n(\lambda)=1+\sum_{i=1}^{3}j_i \quad , \tag{2}$$

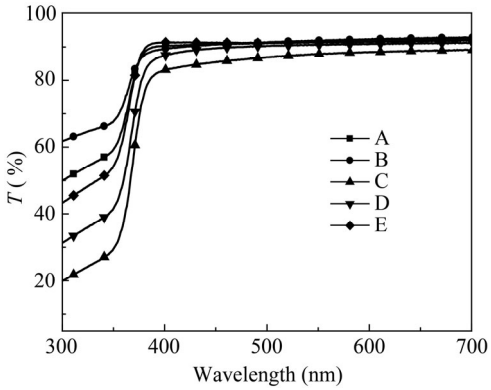

Fig.2 Transmittance spectra of five nano-ZnO thin films

where j_i (i=1, 2 and 3) are the contributions of $\alpha(\lambda')$ to the refractive index in the wavelength regions of $\lambda'<\lambda_1'$, $\lambda_1'\sim\lambda_2'$ and $\lambda'>\lambda_2'$, respectively. For a direct band gap semiconductor near the band edge, in the range of $\lambda'<\lambda_1'$, $\alpha(\lambda')$ is given by[21]

$$\alpha(\lambda')=\mathrm{A}(\frac{hc}{\lambda'}-E_{\mathrm{g}})^{1/2}, \tag{3}$$

where A is a constant, h and c represent Planck's constant and light speed, respectively, and E_{g} is the band gap of a semiconductor. In the region of $\lambda'<\lambda_1'$, assuming there is only one absorption band and $\alpha(\lambda')$ satisfies Eqs.(2) and (1), j_1 can be calculated according to the following three cases, $hc/\lambda'-E_{\mathrm{g}}>0$, $hc/\lambda'-E_{\mathrm{g}}=0$ and $hc/\lambda'-E_{\mathrm{g}}<0$. In Ref.[21], the equations to calculate j_1 in the above three cases are given, but there are some errors. So here we need to correct the equations. The results are as follows.

If $hc/\lambda'-E_{\mathrm{g}}>0$, j_1 should be

$$j_1=-\frac{\mathrm{A}\lambda}{4\pi^2}\sqrt{\frac{hc}{\lambda}-E_{\mathrm{g}}}\times\ln\left|\frac{\sqrt{\frac{hc}{\lambda'}-E_{\mathrm{g}}}-\sqrt{\frac{hc}{\lambda}-E_{\mathrm{g}}}}{\sqrt{\frac{hc}{\lambda'}-E_{\mathrm{g}}}+\sqrt{\frac{hc}{\lambda}-E_{\mathrm{g}}}}\right|-$$

$$\frac{\mathrm{A}\lambda}{2\pi^2}\sqrt{\frac{hc}{\lambda}+E_{\mathrm{g}}}\times\arctan\frac{\sqrt{\frac{hc}{\lambda'}-E_{\mathrm{g}}}}{\sqrt{\frac{hc}{\lambda'}+E_{\mathrm{g}}}}+\frac{\mathrm{A}\lambda}{2\pi^2}\sqrt{\frac{hc}{\lambda}+E_{\mathrm{g}}}\times\frac{\pi}{2}. \tag{4}$$

If $hc/\lambda'-E_{\mathrm{g}}=0$, j_1 is given by

$$j_1 = -\frac{A\lambda}{2\pi^2}\sqrt{\frac{hc}{\lambda}+E_g}\arctan\frac{(\frac{hc}{\lambda_1'}-E_g)}{\sqrt{\frac{hc}{\lambda}+E_g}}+\frac{A\lambda}{2\pi^2}\sqrt{\frac{hc}{\lambda}+E_g}\frac{\pi}{2}. \quad (5)$$

And if $hc/\lambda' - E_g < 0$, j_1 is given by

$$j_1 = -\frac{A\lambda}{2\pi^2}\sqrt{E_g-\frac{hc}{\lambda}}\arctan\frac{(\frac{hc}{\lambda_1'}-E_g)}{\sqrt{E_g-\frac{hc}{\lambda}}}-\frac{A\lambda}{2\pi^2}\sqrt{E_g-\frac{hc}{\lambda}}\times\arctan\frac{(\frac{hc}{\lambda_1'}-E_g)}{\sqrt{\frac{hc}{\lambda}+E_g}}+\frac{A\lambda}{2\pi^2}\sqrt{\frac{hc}{\lambda}+E_g}\frac{\pi}{2} \quad . \quad (6)$$

In the regions of $\lambda_1' \sim \lambda_2'$ and $\lambda' > \lambda_2'$, the equations to calculate j_2 and j_3 are the same as those in Ref.[21]. The extinction coefficients, real and imaginary components of the dielectric constants of nano-ZnO thin films can be obtained according to Ref.[21].

Fig.3 shows the absorption coefficients of nano-ZnO thin films as a function of wavelength. The absorption coefficients in UV range are larger than those in visible range, which is similar to the cases at higher temperature annealing[21-23]. Whatever in UV or visible range, the sample B has the maximum absorption coefficient at the same wavelength, while the sample C has the minimum one. The other three samples almost have the same absorption coefficient at the same wavelength. The absorption is related to the defects in nano-ZnO thin films. After 30 h annealing at 100 °C, the nano-ZnO thin films become stable[29]. The interstitial zinc (Zn_i) will decrease and interstitial oxygen (O_i) will increase. The thicknesses of samples B and C are the minimum and maximum, respectively. The density of O_i in sample B is larger than that in sample C basically. We also calculate the extinction coefficients of nano-ZnO thin films with various wavelengths and the results are shown in Fig.4.

Fig.5 shows the refractive indices of nano-ZnO thin films. In visible range, the refractive indices increase slowly with wavelength increasing. There is a slight abnormal dispersion in these low-temperature processed nano-ZnO thin films. Our result is similar to that in Ref.[22], but different from that at higher temperature annealing[21,23,25]. For our result, in visible range, the refractive indices of samples A, B, C, D and E are in the ranges of 1.71—1.64, 1.81—1.73, 1.56—1.51, 1.57—1.52 and 1.74—1.61, respectively. At 500 nm, the refractive indices of the samples B, D(E), A(C) are around 1.75, 1.63 and 1.52, respectively, while at 700 nm, those are around 1.85, 1.73 and 1.59, respectively.

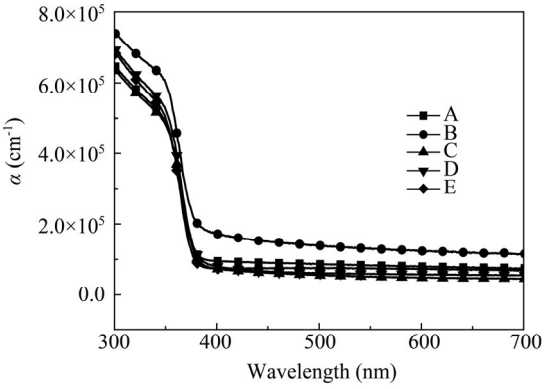

Fig.3 Absorption coefficients of nano-ZnO thin films as a function of wavelength

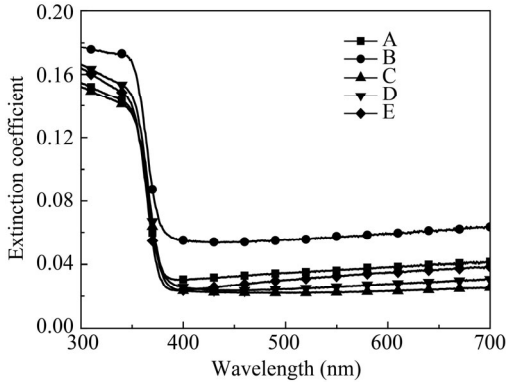

Fig.4 Extinction coefficients of nano-ZnO thin films

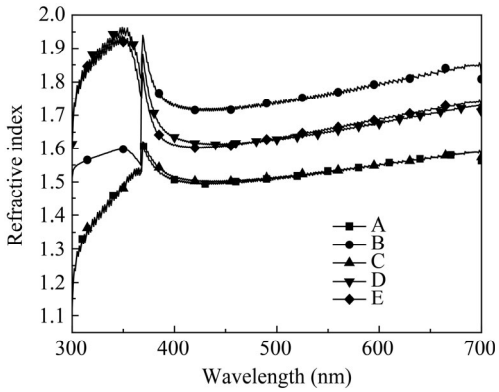

Fig.5 Refractive indices of nano-ZnO thin films as a function of wavelength

In UV range, the refractive indices increase with the wavelength increasing. But the refractive indices show complicated change near the absorption edge, especially for samples A, B and C. Among the five samples, D and E have the maximum refractive indices in UV range. But the maximum refractive index (1.95) of nano-ZnO thin films in UV range at low temperature annealing is much lower than that of films annealed at high temperature[21,25]. The reason is that the refractive index is closely related to the polarizbility of ions and the local

field (defects) inside the materials[21].

Figs.6 and 7 show the real and imaginary components of the complex dielectric constants of nano-ZnO thin films, respectively. The real components follow the same pattern as the refractive indices changing with wavelength. The imaginary components are lower than the real components. For the imaginary components, in UV range, the values are almost constants. And in visible range, the imaginary components slowly increase with wavelength.

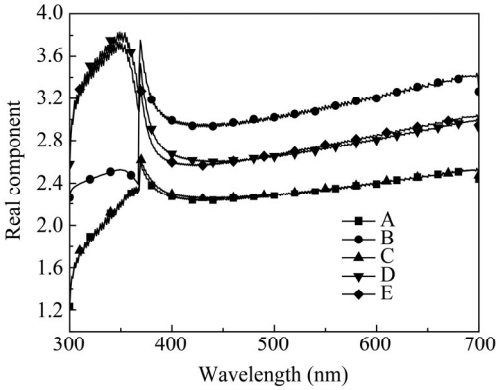

Fig.6 Real components of the complex dielectric constants of nano-ZnO thin films

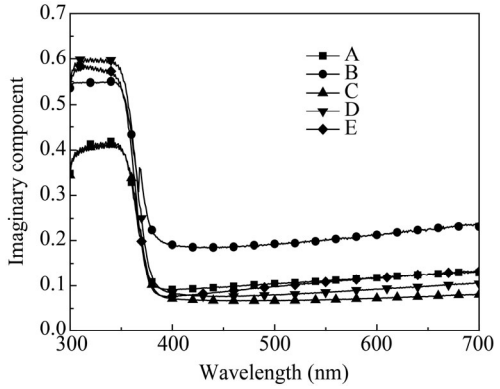

Fig.7 Imaginary components of the complex dielectric constants of nano-ZnO thin films

In this paper, ZnO nanoparticles with sizes of 10—16 nm were prepared by the sol-gel method. By spin-coating, nano-ZnO thin films on quartz substrates were obtained. The SEM and transmission spectra of these films were measured. The theory based on Kramers-Kronig relationship to calculate the refractive indices of thin films in Ref.[21] is corrected. The absorption coefficients, extinction coefficients, refractive indices, real and imaginary components of the dielectric constants of nano-ZnO thin films are calculated. In visible range, the refractive indices indicate a slight abnormal dispersion, which is different from those annealed at high temperature. In UV range, the refractive indices increase with wavelength increasing. But the refractive indices show complicated change near the absorption edge. The maximum refractive index (1.95) of nano-ZnO thin films in UV range at low temperature annealing is much lower than that of films annealed at high temperature. We think that the absorption and refractive indices are closely related to the defects in nano-ZnO thin films. The main reason may be that O_i is different for the nano-ZnO thin films annealed at low temperature and at high temperature.

References

[1] S. Dutta, S. Chattopadhyay, A. Sarkar, M. Chakrabarti, D. Sanyal and D. Jana, Prog. Mater. Sci. **54**, 89 (2009).

[2] E. S. P. Leong and S. F. Yu, Adv. Mater. **18**, 1685 (2006).

[3] Shabnam, C. R. Kant and P. Arun, J. Lumin. **132**, 1744 (2012).

[4] J. M. Bian, W. F. Liu, J. C. Sun and H. Liang, J. Mater. Proc. Tech. **184**, 451 (2007).

[5] D. D. Wang, G. Z. Xing, M. Gao, L. Yang, J. Yang and T. Wu, J. Phys. Chem. C **115**, 22729 (2011) .

[6] O. Yilmazoglu, J. P. Biethan, A. Evtukh, M. Semenenko, D. Pavlidis, H. L. Hartnagel and V. Litovchenko, Appl. Surf. Sci. **258**, 4990 (2012).

[7] V. A. Karpyna, A. A. Evtukh, M. O. Semenenko, V. I. Lazorenko, G. V. Lashkarev, V. D. Khranovskyy, R. Yakimova and D. A. Fedorchenko, Microelectron. J. **40**, 229 (2009).

[8] H. Ohta, M. Kamiya, T. Kamiya, M. Hirano and H. Hosono, Thin Solid Films **445**, 317 (2003).

[9] S. S. Shinde and K. Y. Rajpure, J. Alloys. Comp. **522**, 118 (2012).

[10] T. H. Moon, M. C. Jeong, W. Lee and J. M. Myoung, Appl. Surf. Sci. **240**, 280 (2005).

[11] D. T. Phan and G. S. Chung, Sens. Actuators B **161**, 341 (2012).

[12] L. X. Zhang, J. H. Zhao, H. Q. Lu, L. M. Gong, L. Li, J. F. Zheng, H. Li and Z. P. Zhu, Sens. Actuators B **160**, 364 (2011).

[13] S. Hemmati, A. A. Firooz, A. A. Khodadadi and Y. Mortazavi, Sens. Actuators B **160**, 1298 (2011).

[14] D. Karageorgopoulos, E. Stathatos and E. Vitoratos, J. Power Sources **219**, 9 (2012).

[15] K. Schwanitz, S. Klein, T. Stolley, M. Rohde, D. Severin and R. Trassl, Sol. Energy Mater. Sol. Cells **105**, 187 (2012).

[16] D. R. Bekci, A. Karsli, A. C. Cakir, H. Sarica, A. Guloglu, S. Gunes and S. Erten-Ela, Appl. Energy **96**, 417 (2012).

[17] C. Martínez, M. L. Canle, M. I. Fernández, J. A. Santaballa and J. Faria, Appl. Catal. B: Environ. **102**, 563 (2011).

[18] Y. L. Lai, M. Meng, Y. F. Yu, X. T. Wang and T. Ding, Appl. Catal. B: Environ. **105**, 335 (2011).

[19] W. H. Hu, Y. S. Liu, H. B. Yang, X. Q. Zhou and C. M.

Li, Biosens. Bioelectron. **26**, 3683 (2011).
[20] Y. H. Wang, W. J. Duan, Z. L. Wu, D. Zheng, X. U. Zhou, B. Y. Zhou, L. J. Dai and Y. S. Wang, J. Lumin. **132**, 1885 (2012).
[21] S. W. Xue, X. T. Zu, W. L. Zhou, H. X. Deng, X. Xiang, L. Zhang and H. Deng, J. Alloys Comp. **448**, 21 (2008).
[22] E. Senadm, H. Kavak and R. Esen, J. Phys. Condens. Matter **18**, 6391 (2006).
[23] B. Huang, J. Li, Y. B. Wu, D. H. Guo and S. T. Wu, Mater. Lett. **62**, 1316 (2008).
[24] S. W. Xue, X. T. Zu, W. G. Zheng, H. X. Deng and X. Xiang, Physica B **381**, 209 (2006).
[25] J. Lv, K. Huang, X. Chen, J. Zhu, C. Cao, X. Song and Z. Sun, Opt. Commun. **284**, 2905 (2011).
[26] H. Segawa, H. Sakurai, R. Izumi, T. Hayashi, T. Yano and S. Shibata, J. Mater. Sci. **46**, 3537 (2011).
[27] X. C. Bao, Y. Yang, A. L. Yang, N. Wang, T. Wang, Z. K Du, C. P. Yang, S. G. Wen and R. Q. Yang, Mater. Sci. Eng. B **178**, 263 (2013).
[28] X. C. Bao, A. L. Yang, Y. Yang, T. Wang, L. Sun, N. Wang and L. L. Han, Physica B **432**, 1 (2014).
[29] A. L. Yang, Y. Yang, Z. Z. Zhang, X. C. Bao, R. Q. Yang, S. P. Li and L. Sun, Sci. China Tech. Sci. **56**, 25 (2013).